

Supplement of Atmos. Chem. Phys. Discuss., 15, 19405–19445, 2015  
<http://www.atmos-chem-phys-discuss.net/15/19405/2015/>  
doi:10.5194/acpd-15-19405-2015-supplement  
© Author(s) 2015. CC Attribution 3.0 License.



*Supplement of*

## **Continuous measurements at the urban roadside in an Asian Megacity by Aerosol Chemical Speciation Monitor (ACSM): particulate matter characteristics during fall and winter seasons in Hong Kong**

**C. Sun et al.**

*Correspondence to:* C. K. Chan (keckchan@ust.hk)

The copyright of individual parts of the supplement might differ from the CC-BY 3.0 licence.

## 1 **Supporting Material**

### 3 **1. Sampling set-up**

4 Ambient air was sampled through a PM<sub>2.5</sub> cyclone on the rooftop (approximately 3m above ground  
5 level) of an air conditioned sampling shelter at a flow rate of 3.1 L/min, with 0.1 L/min drawn by  
6 the ACSM. The sampled air passed through a Nafion dryer (PD-200T-12MSS, Perma Pure LLC)  
7 before going into the ACSM. Ionization efficiency (IE) calibrations were performed at least once  
8 per month during the first three months with DMA-size-selected ( $D_m=350\text{nm}$ ) pure ammonium  
9 nitrate particles [Jayne *et al.*, 2000; Lee *et al.*, 2015, submitted]. A HEPA filter was installed in-  
10 line before the ACSM for one- to three hours (filter time) per month to determine the detection  
11 limits (DL) of the ACSM, which are defined as three times the standard deviations of the  
12 concentrations of all species during the filter period. Data points falling below their corresponding  
13 detection limit were set to zero in our analysis (Table S1). All mass concentrations were  
14 determined at ambient temperature and pressure and presented in local time.

### 16 **2. Data Treatment**

17 The ammonium RIE of 4.57 and sulfate RIE of 1.2 were chosen based on the average from five IE  
18 calibrations, while the default RIE values of 1.1 for nitrate, 1.3 for chloride and 1.4 for organics  
19 were used [Allan *et al.*, 2003; Jimenez *et al.*, 2003]. The influence of RH in this study is considered  
20 minor as a Nafion dryer was used to keep the sampling line RH consistently below 30%.  
21 Middlebrook *et al.* [2012] developed an equation based to aerosol composition to estimate the  
22 collection efficiency (CE). Under the dry conditions used in our sampling, the Middlebrook  
23 parameterization suggests a CE of ~45-50% based on the measured inorganic constituents  
24 (Middlebrook *et al.*, 2012). However, the NR-PM<sub>1</sub> concentration of the majority of data points  
25 (~83%), if calculated with a CE of 0.45, would exceed the PM<sub>2.5</sub> concentration measured by TEOM  
26 which indicates an underestimation of CE. Therefore, the Middlebrook result does not seem  
27 appropriate for this study as the dominance of organic compounds (58.2% of NR-PM<sub>1</sub>) at the  
28 measurement site could hinder the complete efflorescence of particles in the drier and reduce the  
29 particle bounce effect, thus increasing the particle collection efficiency.

30 A CE of 0.8 was chosen based on the comparison of the NR-PM<sub>1</sub> measurements and PM<sub>2.5</sub>  
31 measured independently by HKEPD. The average ratio of NR-PM<sub>1</sub> to PM<sub>2.5</sub> (0.59; Figure S1) is  
32 consistent with the results in previous studies that NR-PM<sub>1</sub> contributes 56%-64% of PM<sub>2.5</sub>  
33 assuming that NR-PM<sub>1</sub> approximately equals the difference between PM<sub>2.5</sub> and elemental carbon  
34 (EC) in PM<sub>2.5</sub> [Cheng *et al.*, 2006; Lee *et al.*, 2006].

### 35 **3. PMF analysis on Organic Spectra**

36 In this study, PMF input mass spectra were limited to a maximum  $m/z$  of 110 because the signal  
37 uncertainty at higher  $m/z$  values was large due to low ion transmission efficiency and significant  
38 interferences from the internal standard of naphthalene at  $m/z$  127-129 [Ng *et al.*, 2011; Sun *et al.*,  
39 2013]. PMF was run in “exploration” mode with  $f_{\text{peak}}$  changing from -1 to 1 in steps of 0.2 and  
40 the P value (the number of factor) from 1 to 6. PMF analysis procedures followed those in Zhang  
41 *et al.* [2005, 2011].

42 A 4-factor solution is thought to be optimal. First, a 3-factor solution resolves hydrocarbon-like  
43 OA (HOA) incorrectly (Figure S2) with excess  $m/z$  44 fractional intensity ( $f_{44}=5\%$ ) and a rather  
44 poor correlation with NO<sub>x</sub>, with a Pearson’s R value ( $R_{\text{pr}}$ ) of 0.43 (Table S2). On the other hand,  
45 a 5-factor solution resolves one unknown factor (Factor 1) which shows very similar variations in  
46 time series as Factor 4 ( $R_{\text{pr}}=0.80$ ; Figure S3). The 4-factor solution yields  $Q/Q_{\text{exp}}=0.8$  and better  
47 differentiation among the factor time series ( $R_{\text{pr}} < 0.6$ ; Figure S4). The four factors also correlate  
48 well with associated inorganics and external tracers [NO<sub>3</sub>, SO<sub>4</sub>, NH<sub>4</sub>, NO<sub>x</sub>; Zhang *et al.*, 2005a,  
49 2011; Ulbrich *et al.*, 2009], e.g. HOA with NO<sub>x</sub>, SV-OOA with NO<sub>3</sub>, LV-OOA with SO<sub>4</sub> and NH<sub>4</sub>  
50 (Table S4). Furthermore, the mass spectra of the four factors are similar (all un-centered R  
51 ( $R_{\text{uc}} > 0.80$ ) to corresponding reference mass spectra from the AMS MS database [Ulbrich, I. M.,  
52 Lechner, M., and Jimenez, J. L., AMS Spectral Database, url: [http://cires.colorado.edu/jimenez-](http://cires.colorado.edu/jimenez-group/AMSsd)  
53 [group/AMSsd](http://cires.colorado.edu/jimenez-group/AMSsd); Ulbrich *et al.*, 2009], as shown in next section. With the 4-factor solution, the  
54 variation of  $f_{\text{peak}}$  had little impact on the value of  $Q/Q_{\text{exp}}$ , while HOA and low-volatile OOA at  
55  $f_{\text{peak}}=0$  showed the highest correlations with both NO<sub>x</sub> and SO<sub>4</sub>, when compared with solutions  
56 using other rotational values (Table S5). Therefore, a 4-factor solution with  $f_{\text{peak}}=0$  was chosen.

#### 57 Hydrocarbon-like Organic Aerosol (HOA)

58 The mass spectrum of HOA (Figure 4) is dominated by a homologous series of alkyl fragments  
59 separated by a CH<sub>2</sub> (*m/z* 14) unit: the C<sub>*n*</sub>H<sub>2*n*-1</sub><sup>+</sup> ion series (*m/z* 27, 41, 55, 69, 83, 97), typical of  
60 cycloalkanes or unsaturated hydrocarbon, which account for 27% of total peak intensity in the  
61 HOA spectrum. The other prominent group is the C<sub>*n*</sub>H<sub>2*n*+1</sub><sup>+</sup> ion series (*m/z* 29, 43, 57, 71, 85, 99),  
62 typical of alkanes and accounting for 26% of the total peak intensity [McLafferty and Turecek,  
63 1993; Ng *et al.*, 2011; Li *et al.*, 2012]. This mass spectrum is very similar to the standard HOA  
64 spectrum with R<sub>uc</sub> of 0.92, and its fractions of C<sub>*n*</sub>H<sub>2*n*-1</sub><sup>+</sup> and C<sub>*n*</sub>H<sub>2*n*+1</sub><sup>+</sup> (27%, 26%) are consistent  
65 with standard ones (=28%, 27%) [Ng *et al.*, 2011]. This HOA spectrum is also consistent with that  
66 resolved by HR-ToF-AMS at the HKUST Supersite on the dominance of saturated C<sub>*x*</sub>H<sub>*y*</sub>-type  
67 ions, most notably at *m/z* 43 and 57 [Lee *et al.*, 2013].

#### 68 Cooking Organic Aerosol (COA)

69 The most prominent ions of the resolved COA profile at MK were *m/z* 41 (mainly C<sub>2</sub>HO<sup>+</sup>, C<sub>3</sub>H<sub>5</sub><sup>+</sup>)  
70 and *m/z* 55 (mainly C<sub>3</sub>H<sub>3</sub>O<sup>+</sup>, C<sub>4</sub>H<sub>7</sub><sup>+</sup>). Ratios of *m/z* 41/43 =1.8 and *m/z* 55/57=2.2, which are  
71 distinctly larger than that of HOA at 0.73 and 0.76 respectively (Figure 4); such ratios have been  
72 widely reported for COA in AMS and ACSM studies. For example, Lanz *et al.* [2010] reported  
73 ratios of *m/z* 41/43 and *m/z* 55/57 of 0.5 and 0.4 in HOA, and 1.2 and 1.2 in COA, respectively,  
74 while Sun *et al.* [2013] reported 0.5 for these two ratios in HOA and 2.3 for those in COA,  
75 respectively.

#### 76 Oxygenated Organic Aerosol

77 LV-OOA is characterized by the prominent *m/z* 44 ion (mainly CO<sub>2</sub><sup>+</sup>) and minor C<sub>*n*</sub>H<sub>2*n*-1</sub> and  
78 C<sub>*n*</sub>H<sub>2*n*+1</sub> ion series generated by saturated alkanes, alkenes and cycloalkanes. The LVOOA spectra  
79 correlated well with the standard spectra of LV-OOA (Figure 4) with a R<sub>uc</sub> of 0.97. Furthermore,  
80 its time series is comparable to that of SO<sub>4</sub><sup>2-</sup> with a R<sub>pr</sub> of 0.86 (Figure 1), consistent with reports  
81 in the literature [DeCarlo *et al.*, 2010; He *et al.*, 2011; Zhang *et al.*, 2014; Tiitta *et al.*, 2014]. SV-  
82 OOA, which is less oxidized than LV-OOA, is marked by the dominant ions of *m/z* 43 and *m/z* 44  
83 mainly contributed by C<sub>2</sub>H<sub>3</sub>O<sup>+</sup> and CO<sub>2</sub><sup>+</sup>, The mass spectrum of SV-OOA closely resembles that of  
84 'standard' SV-OOA with a R<sub>uc</sub> of 0.87 (Figure 3). Its time series also follows that of nitrate  
85 (R<sub>pr</sub>=0.63, Figure 1), another secondary and semi-volatile species.

87 **Tables**

88

89 **Table S1.** Summary for monthly detection limits of NR-PM<sub>1</sub> species (SO<sub>4</sub>, NO<sub>3</sub>, NH<sub>4</sub>, Chl and Org)

Species $\mu\text{g}/\text{m}^3$	September	October	November	December
SO <sub>4</sub>	0.22	0.04	0.05	0.07
NO <sub>3</sub>	0.04	0.01	0.02	0.05
NH <sub>4</sub>	0.07	0.06	0.12	0.11
Chl	0.02	0.03	0.02	0.02
Org	0.69	0.17	0.28	0.34

90

91 **Table S2.** Correlation coefficients ( $R_{pr}$ ) between resolved factors and SO<sub>4</sub>, NO<sub>3</sub>, NH<sub>4</sub> and NO<sub>x</sub> under solution of 3  
92 factors with fPeak=0.

Pearson R	SO <sub>4</sub>	NO <sub>3</sub>	NH <sub>4</sub>	NO <sub>x</sub>
Factor1	0.80	0.66	0.85	0.25
Factor2	0.07	0.13	0.08	0.55
Factor3	0.40	0.67	0.57	0.43

93

94 **Table S3.** Correlation coefficients ( $R_{pr}$ ) between resolved factors and SO<sub>4</sub>, NO<sub>3</sub>, NH<sub>4</sub> and NO<sub>x</sub> under solution of 5  
95 factors with fPeak=0.

Pearson R	SO <sub>4</sub>	NO <sub>3</sub>	NH <sub>4</sub>	NO <sub>x</sub>
Factor1	0.28	0.48	0.38	0.31
Factor2	0.85	0.57	0.86	0.25
Factor3	-0.01	0.13	0.04	0.48
Factor4	0.54	0.71	0.70	0.30
Factor5	<b>0.16</b>	<b>0.33</b>	<b>0.25</b>	<b>0.68</b>

96

97 **Table S4.** Correlation coefficients ( $R_{pr}$ ) between resolved factors and  $SO_4$ ,  $NO_3$ ,  $NH_4$  and  $NO_x$  under solution of 4  
 98 factors with fPeak=0.

<b>Pearson R</b>	<b><math>SO_4</math></b>	<b><math>NO_3</math></b>	<b><math>NH_4</math></b>	<b><math>NO_x</math></b>
<b>LV-OOA</b>	0.86	0.63	0.88	0.21
<b>SV-OOA</b>	0.39	0.63	0.55	0.39
<b>COA</b>	0.05	0.11	0.06	0.42
<b>HOA</b>	0.25	0.48	0.38	0.70

99  
 100 **Table S5.** Correlation coefficients between resolved factors and associated tracer ( $SO_4$ ,  $NO_3$  and  $NO_x$ ) on time series,  
 101 and corresponding standard mass spectra.

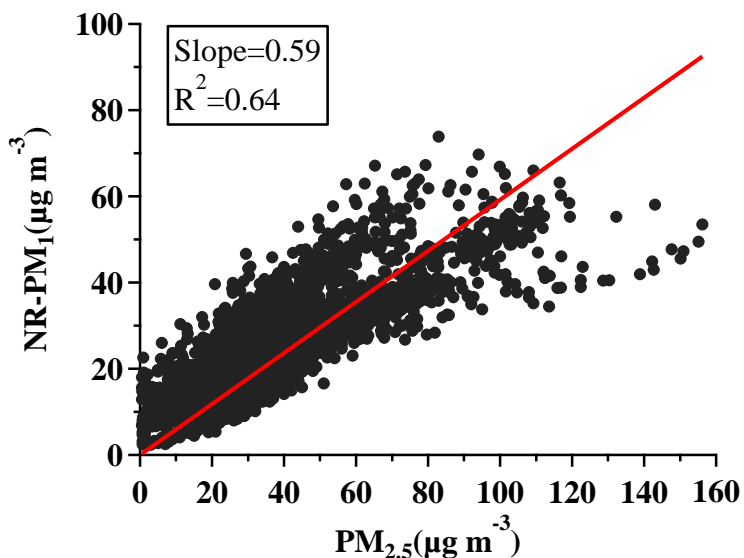
<b>fPeak</b>	<b>-0.4</b>	<b>-0.2</b>	<b>0</b>	<b>+0.2</b>	<b>+0.4</b>
<b>Correlation with associated tracer (<math>R_{pr}</math>)</b>					
<b>HOA &amp; <math>NO_x</math></b>	0.64	0.65	0.70	0.63	0.63
<b>LV-OOA &amp; <math>SO_4</math></b>	0.82	0.85	0.86	0.84	0.80
<b>SV-OOA &amp; <math>NO_3</math></b>	0.64	0.63	0.63	0.64	0.64
<b>Correlation with standard mass spectra (<math>R_{uc}</math>)</b>					
<b>HOA</b>	0.94	0.94	0.92	0.90	0.88
<b>COA</b>	0.77	0.77	0.84	0.76	0.75
<b>LV-OOA</b>	0.98	0.98	0.97	0.97	0.97
<b>SV-OOA</b>	0.83	0.85	0.87	0.78	0.84

102  
 103 **Table S6.** Correlation coefficients ( $R_{pr}$ ) between HOA concentration and  $NO_x$ , CO and VOCs (n-Pentane, i-Pentane,  
 104 Toluene, Benzene).

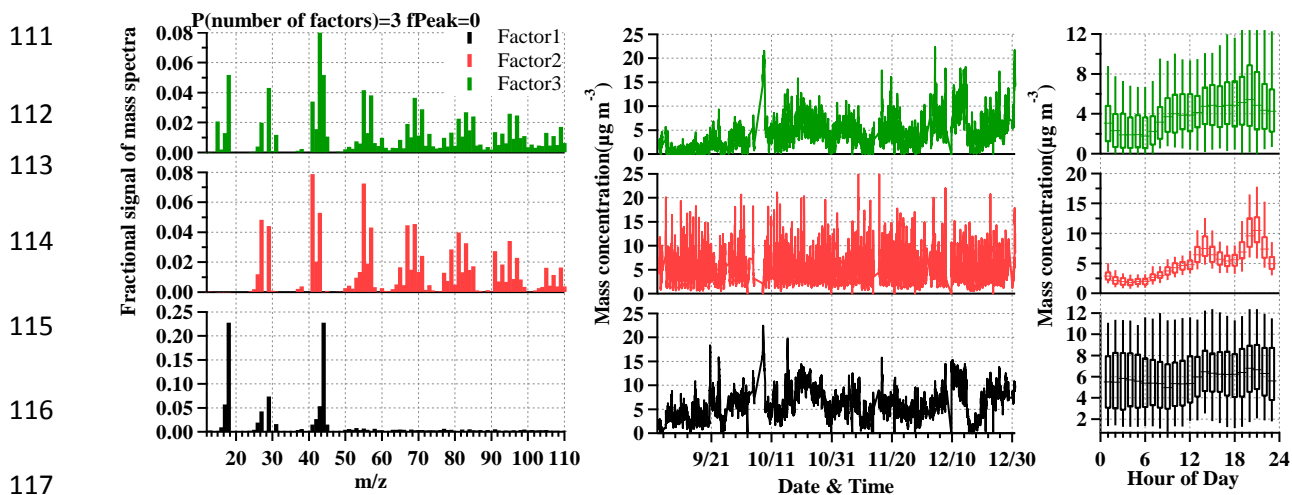
<b>Gas/VOCs</b>	<b><math>R_{pr}</math> with HOA</b>
<b><math>NO_x</math></b>	0.69
<b>CO</b>	0.62
<b>n-Pentane</b>	0.61
<b>i-Pentane</b>	0.57
<b>Toluene</b>	0.55
<b>Benzene</b>	0.56

105

106

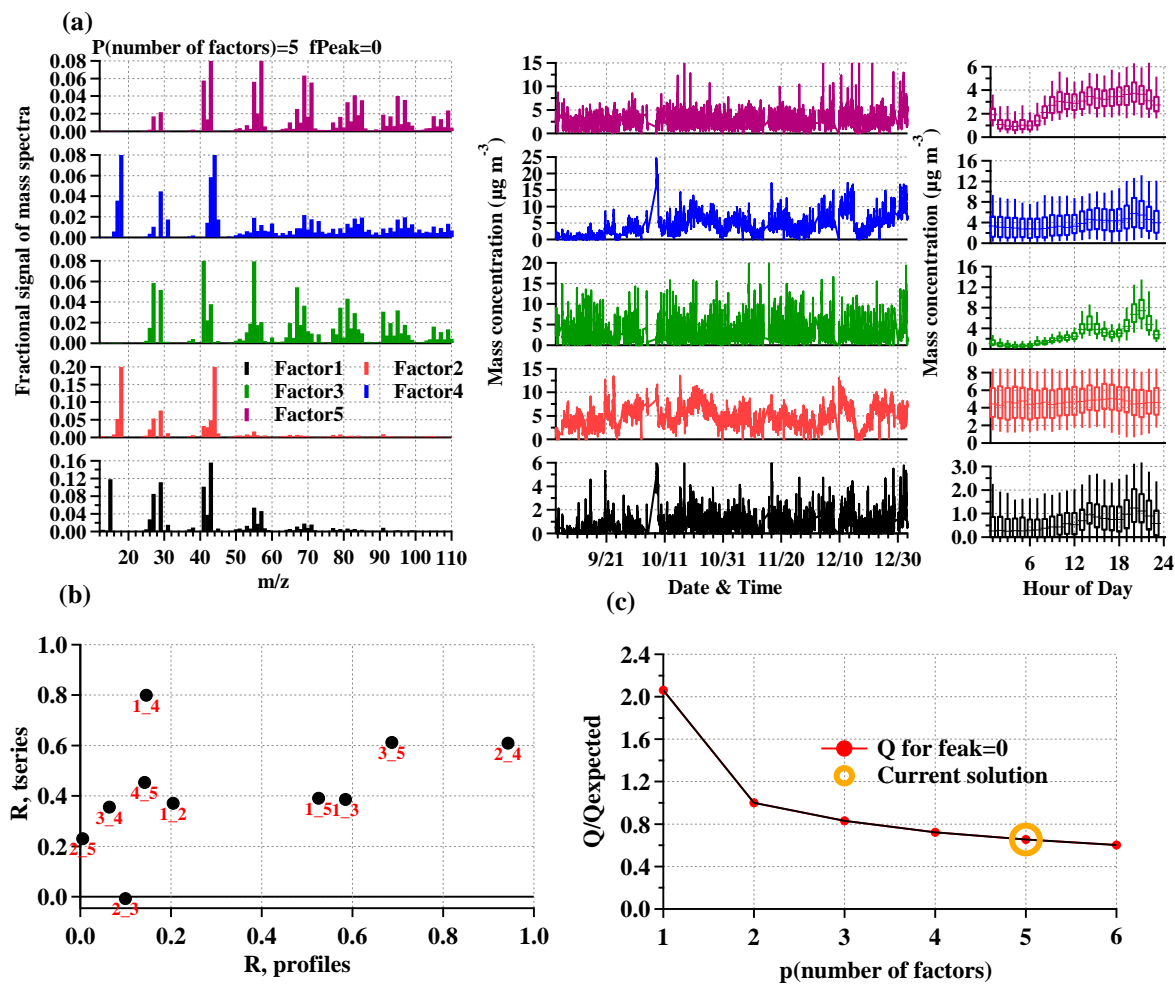


108  
 109 **Figure S1.** (y) NR-PM<sub>1</sub> concentration measured by ACSM versus (x) PM<sub>2.5</sub> measured by TEOM during the entire  
 110 study period.

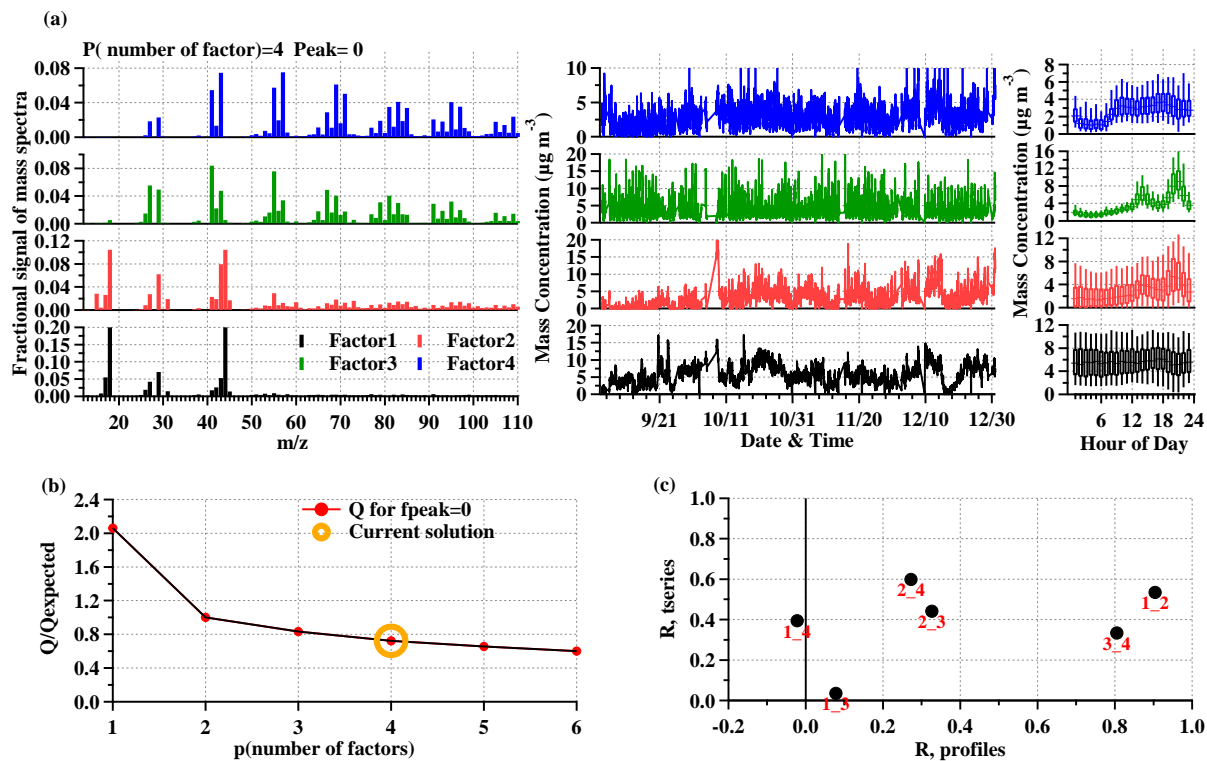


111  
 112  
 113  
 114  
 115  
 116  
 117 **Figure 2S.** The mass spectra, time series and diurnal pattern for 3 factors with fPeak=0

118  
 119  
 120  
 121

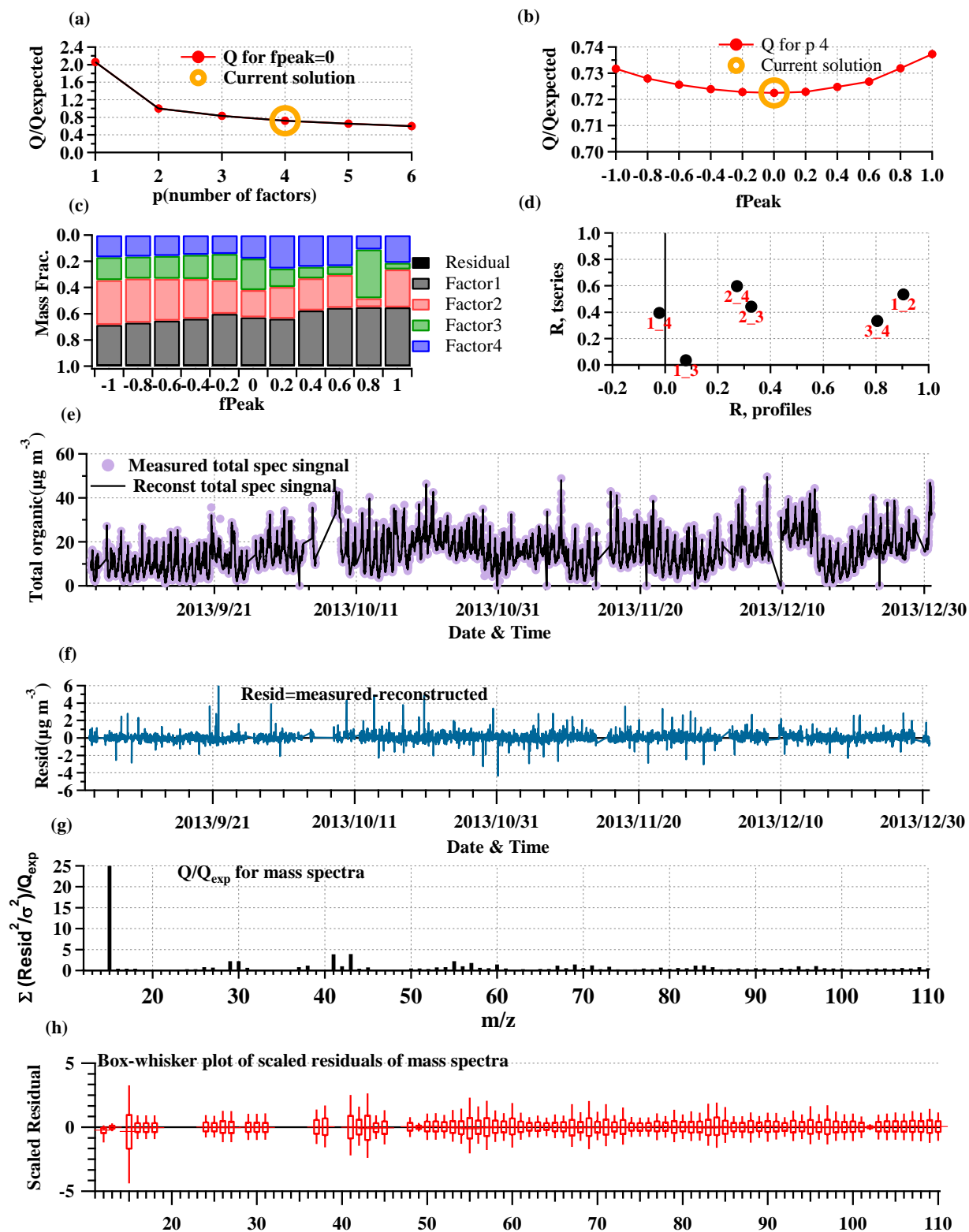


124 **Figure 3S.** (a) The mass spectra, time series, and diurnal pattern for 5 factors with fPeak=0, (b) correlation between  
 125 mass spectra profile or time series profiles of each two factors, and (c)  $Q/Q_{\text{exp}}$  variation as a function of  
 126 factors.



127  
 128 **Figure 4S.** (a) The mass spectra, time series and diurnal pattern for 4 factors with fPeak=0, (b) correlation between  
 129 mass spectra profile or time series profiles of each two factors, and (c)  $Q/Q_{\text{exp}}$  variation as a function of number of  
 130 factors.

131  
 132  
 133

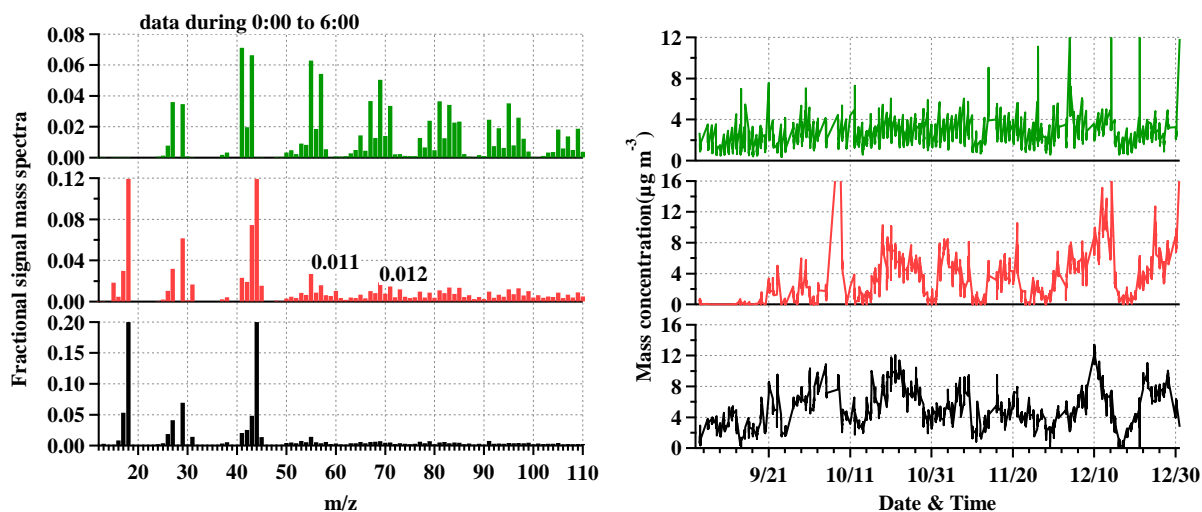


134

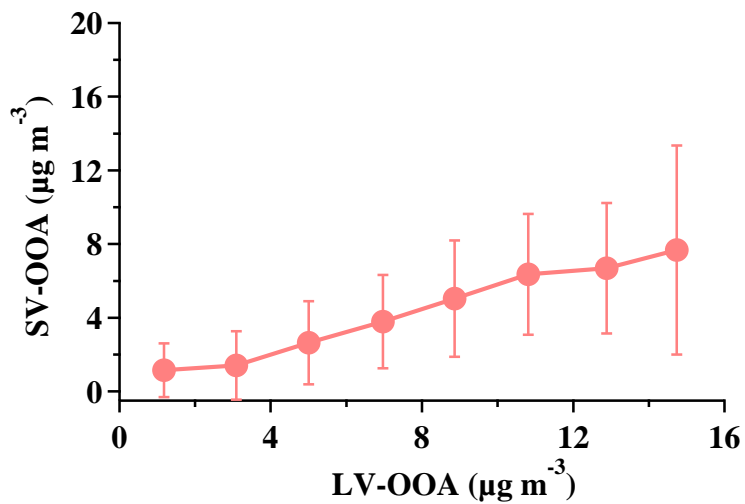
135 **Figure 5S.** PMF diagnostics for 4 factors with  $f_{\text{Peak}}=0$ .

136

137



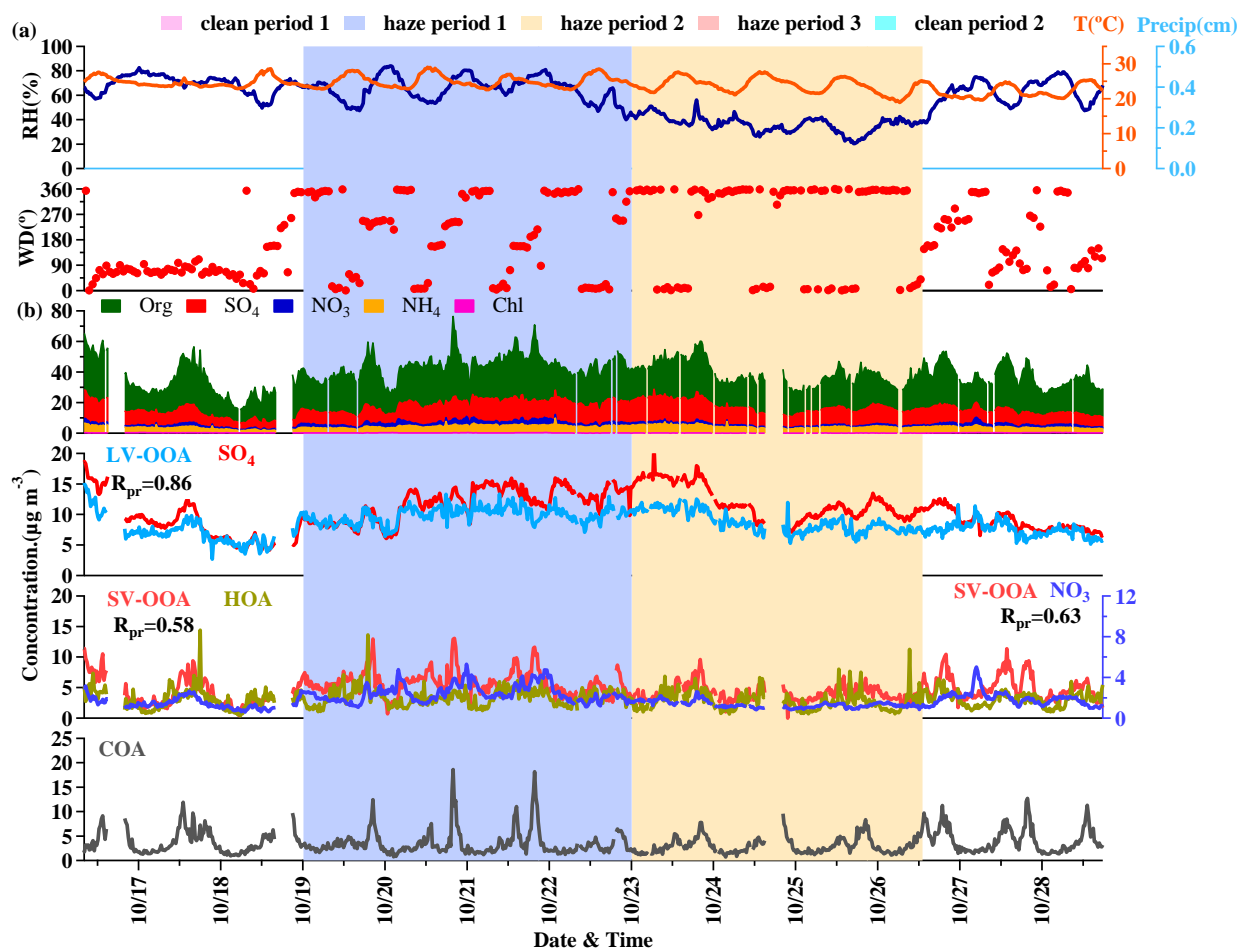
138 **Figure S6.** The mass spectra and time series resolved by PMF based on data with little COA (0:00 -6:00).



139

140 **Figure S7.** Variation of average concentration of SV-OOA binned by LV-OOA concentration with a step of 2 µg/m<sup>3</sup>  
141 as a function of binned LV-OOA concentration.

142



143

144 **Figure S8.** Overview of temporal variation of (a) meteorological factors (Relative humidity, Temperature and  
 145 Precipitation) and (b) non-refractory PM<sub>1</sub> species (Org, SO<sub>4</sub>, NO<sub>3</sub>, NH<sub>4</sub> and Chl) and organic aerosol components  
 146 (LVOOA, SVOOA, HOA and COA) during haze period 1 (H1) and haze period 2 (H2).

147

148

149

150

151

152

153

154

155

156

## 157 References

158 Allan, J. D., Jimenez, J. L., Williams, P. I., Alfarra, M. R., Bower, K. N., Jayne, J. T., Coe, H.  
159 and Worsnop, D. R.: Quantitative sampling using an Aerodyne aerosol mass spectrometer 1.  
160 Techniques of data interpretation and error analysis, *J. Geophys. Res.*, 108, 4090,  
161 doi: 10.1029/2002jd002358, 2003.

162 Cheng, Y., Ho, K. F., Lee, S. C. and Law, S. W.: Seasonal and diurnal variations of PM1.0,  
163 PM2.5 and PM10 in the roadside environment of hong kong, *China Particuology*, 4, 312-  
164 315, doi: 10.1016/s1672-2515(07)60281-4, 2006.

165 DeCarlo, P. F., Ulbrich, I. M., Crouse, J., de Foy, B., Dunlea, E. J., Aiken, A. C., Knapp, D.,  
166 Weinheimer, A. J., Campos, T., Wennberg, P. O. and Jimenez, J. L.: Investigation of the  
167 sources and processing of organic aerosol over the Central Mexican Plateau from aircraft  
168 measurements during MILAGRO, *Atmos. Chem. Phys.*, 10, 5257-5280, doi:10.5194/acp-  
169 10-5257-2010, 2010.

170 He, L. Y., Lin, Y., Huang, X. F., Guo, S., Xue, L., Su, Q., Hu, M., Luan, S. J. and Zhang, Y. H.:  
171 Characterization of high-resolution aerosol mass spectra of primary organic aerosol  
172 emissions from Chinese cooking and biomass burning. *Atmos. Chem. Phys.*, 10, 11535-  
173 11543, doi: 10.5194/acp-10-11535-2010, 2010.

174 Jayne, J. T., Worsnop, D. R., Kolb, C. E., Leard, D., Davidovits, P., Zhang, X. and Smith, K. A.:  
175 Aerosol mass spectrometer for size and composition analysis of submicron particles. *J.*  
176 *Aerosol Sci.*, 29, S111-S112, doi: 10.1016/s0021-8502(98)00158-x, 1998.

177 Jimenez, J. L., Jayne, J. T., Shi, Q., Kolb, C. E., Worsnop, D. R., Yourshaw, I., Seinfeld, J. H.,  
178 Flagan, R. C., Zhang, X. F., Smith, K. A., Morris, J. W. and Davidovits, P.: Ambient aerosol  
179 sampling using the Aerodyne Aerosol Mass Spectrometer, *J. Geophys. Res.*, 108, 8425, doi:  
180 10.1029/2001jd001213, 2003.

181 Lanz, V. A., Alfarra, M. R., Baltensperger, U., Buchmann, B., Hueglin, C. and Prévôt, A. S. H.:  
182 Source apportionment of submicron organic aerosols at an urban site by factor analytical  
183 modelling of aerosol mass spectra, *Atmos. Chem. Phys.*, 7, 1503-1522, doi: 10.5194/acp-7-  
184 1503-2007, 2007.

185 Lanz, V. A., Prévôt, A. S. H., Alfarra, M. R., Weimer, S., Mohr, C., DeCarlo, P. F., Gianini, M.  
186 F. D., Hueglin, C., Schneider, J., Favez, O., D'Anna, B., George, C. and Baltensperger, U.:  
187 Characterization of aerosol chemical composition with aerosol mass spectrometry in Central  
188 Europe: an overview, *Atmos. Chem. Phys.*, 10, 10453-10471, doi: 10.5194/acp-10-10453-  
189 2010, 2010.

190 Lee, B. P., Li, Y. J., Yu, J. Z., Louie, P. K. K. and Chan, C. K.: Physical and chemical  
191 characterization of ambient aerosol by HR-ToF-AMS at a suburban site in Hong Kong  
192 during springtime 2011. *J. Geophys. Res.*, 118, 8625-8639, doi: 10.1002/jgrd.50658, 2013.

193 Lee, B. P., Li, Y. J., Yu, J. Z., Louie, P. K. K. and Chan, C. K.: Characteristics of submicron  
194 particulate matter at the urban roadside in downtown Hong Kong – overview of 4 months of  
195 continuous high-resolution aerosol mass spectrometer (HR-AMS) measurements, *J.*  
196 *Geophys. Res.*, 2015, submitted.

197 Li, Y. J., Yeung, J. W. T., Leung, T. P. I., Lau, A. P. S. and Chan, C. K.: Characterization of  
198 Organic Particles from Incense Burning Using an Aerodyne High-Resolution Time-of-  
199 Flight Aerosol Mass Spectrometer, *Aerosol Sci. Technol.*, 46, 654-665,  
200 doi: 10.1080/02786826.2011.653017, 2012.

201 McLafferty, F. W and Turecek, F.: Interpretation of mass spectra, University Science Books,  
202 Mill Valley, California, 1993.

203 Middlebrook, A. M., Bahreini, R., Jimenez, J. L. and Canagaratna, M. R.: Evaluation of  
204 Composition-Dependent Collection Efficiencies for the Aerodyne Aerosol Mass  
205 Spectrometer using Field Data, *Aerosol Sci. Technol.*, 46, 258-271,  
206 doi: 10.1080/02786826.2011.620041, 2012.

207 Ng, N. L., Herndon, S. C., Trimborn, A., Canagaratna, M. R., Croteau, P. L., Onasch, T. B.,  
208 Sueper, D., Worsnop, D. R., Zhang, Q., Sun, Y. L. and Jayne, J. T.: An Aerosol Chemical

209 Speciation Monitor (ACSM) for Routine Monitoring of the Composition and Mass  
210 Concentrations of Ambient Aerosol, *Aerosol Sci. Technol.*, 45, 780-794,  
211 doi: 10.1080/02786826.2011.560211, 2011.

212 Sun, Y. L., Wang, Z. F., Fu, P. Q., Yang, T., Jiang, Q., Dong, H. B., Li, J. and Jia, J. J.: Aerosol  
213 composition, sources and processes during wintertime in Beijing, China, *Atmos. Chem.*  
214 *Phys.*, 13, 4577-4592, doi:10.5194/acp-13-4577-2013, 2013.

215 Tiitta, P., Vakkari, V., Croteau, P., Beukes, J. P., van Zyl, P. G., Josipovic, M., Venter, A. D.,  
216 Jaars, K., Pienaar, J. J., Ng, N. L., Canagaratna, M. R., Jayne, J. T., Kerminen, V. M.,  
217 Kokkola, H., Kulmala, M., Laaksonen, A., Worsnop, D. R. and Laakso, L.: Chemical  
218 composition, main sources and temporal variability of PM<sub>1</sub> aerosols in southern African  
219 grassland, *Atmos. Chem. Phys.*, 14, 1909—1927, doi: 10.5194/acp-14-1909-2014, 2014.

220 Ulbrich, I. M., Canagaratna, M. R., Zhang, Q., Worsnop, D. R. and Jimenez, J. L.: Interpretation  
221 of organic components from Positive Matrix Factorization of aerosol mass spectrometric  
222 data, *Atmos. Chem. Phys.*, 9, 2891-2918, doi: 10.5194/acp-9-2891-2009, 2009.

223 Zhang, Q., Alfarra, M. R., Worsnop, D. R., Allan, J. D., Coe, H., Canagaratna, M. R. and  
224 Jimenez, J. L.: Deconvolution and Quantification of Hydrocarbon-like and Oxygenated  
225 Organic Aerosols Based on Aerosol Mass Spectrometry, *Environ. Sci. Technol.*, 39, 4938-  
226 4952, doi: 10.1021/es048568l, 2005.

227 Zhang, Q., Jimenez, J. L., Canagaratna, M. R., Ulbrich, I. M., Ng, N. L., Worsnop, D. R. and  
228 Sun, Y.: Understanding atmospheric organic aerosols via factor analysis of aerosol mass  
229 spectrometry: a review, *Analyt. Bioanalyt. Chem.*, 401, 3045-3067, doi: 10.1007/s00216-  
230 011-5355-y, 2011.

231 Zhang, Y. M., Zhang, X. Y., Sun, J. Y., Hu, G. Y., Shen, X. J., Wang, Y. Q., Wang, T. T., Wang,  
232 D. Z. and Zhao, Y.: Chemical composition and mass size distribution of PM<sub>1</sub> at an elevated  
233 site in central east China, *Atmos. Chem. Phys.*, 14, 12237-12249, doi: 10.5194/acp-14-  
234 12237-2014, 2014.

235

236